

Influence of $\text{TiO}_2/\text{Sb}_2\text{O}_3$ ratio on ZnO varistor ceramics

Congchun Zhang*, Yunxiang Hu, Wenzhong Lu, Minghe Cao, Dongxiang Zhou

Department of Solid State Electronics, Huazhong University of Science and Technology, Wuhan 430074, PR China

Received 19 October 2000; received in revised form 16 January 2001; accepted 3 February 2001

Abstract

The influence of $\text{TiO}_2/\text{Sb}_2\text{O}_3$ (Ti/Sb) ratio on the microstructure development and electrical properties of varistor ceramics in $\text{ZnO}-(\text{Bi}_2\text{O}_3-\text{TiO}_2-\text{Sb}_2\text{O}_3)-\text{CoO}-\text{MnO}_2$ system was investigated. Characterization of varistors was performed by XRD, SEM, d.c. degradation behavior, and electrical measurements. It is found that the Ti/Sb ratio greatly influences the microstructure and electrical properties of the ZnO varistor. The specimen with Ti/Sb ratio of 5 has the lowest breakdown field (20V/mm) and improved d.c. degradation behavior. © 2001 Elsevier Science Ltd. All rights reserved.

Keywords: Ceramics; Degradation; Grain-boundary; Varistors; ZnO

1. Introduction

Zinc oxide varistors are ceramic semiconductors devices which have extreme nonlinearity in their current–voltage behavior and thus are widely used for electronic devices. The nonlinear characteristics are attributed to the formation of double Schottky barriers at the zinc oxide grain boundaries.¹

ZnO varistors are formed by sintering mixture of ZnO powders with small amounts of other oxides, such as those of bismuth, antimony, cobalt, manganese, chromium, etc., at a given temperature. Microstructurally, the device is composed of semiconducting ZnO grains, interspersed with second phases which are predominantly bismuth oxide, $\text{Zn}_7\text{Sb}_2\text{O}_{12}$ spinel and $\text{Zn}_2\text{Bi}_3\text{Sb}_3\text{O}_{14}$ pyrochlore composition.¹ The roles of the additives and synergistic effects are only partially understood.

Nowadays, an ever increasing number of varistors is being used for low-voltage applications, such as in automobile electronics and semiconductor electronics. The approaches to reducing the break-down voltage of varistor have included multilayering, thin foil, and thick film techniques.³ Our approach has been to optimize the processing and composition of conventional varistor in order to maximize ZnO grain size.

The addition of Sb_2O_3 or TiO_2 to ZnO varistors has received considerable attention,^{4–6} because they strongly affect microstructure development and electrical behavior

Sb_2O_3 is a powerful grain growth inhibitor of ZnO. The primary effects of antimony on the electrical properties of varistors devices are to increase breakdown voltage because of inhibited grain growth, decrease the leakage current, and increase the nonlinear coefficient.^{4,11} TiO_2 can greatly enhance the grain growth of ZnO, thus widely used in producing low-voltage ZnO varistors. Previous studies have been devoted to the effect of the Sb_2O_3 ⁽⁴⁾ and TiO_2 ⁽⁹⁾ doping on the grain growth and microstructure of ZnO varistors. It was reported that $\text{Bi}_2\text{O}_3/\text{TiO}_2$ doping had an effect on low-voltage varistor.² However, to the best of our knowledge, in a previous study, they are not co-doped with both TiO_2 and Sb_2O_3 . No study has been devoted to the understanding of the influence of $\text{TiO}_2/\text{Sb}_2\text{O}_3$ ratio on the microstructure development and subsequent electrical behavior.

In present work, the influences of $\text{TiO}_2/\text{Sb}_2\text{O}_3$ ratio on the microstructure and electrical characteristic of varistor ceramics in $\text{ZnO}-(\text{Bi}_2\text{O}_3-\text{TiO}_2-\text{Sb}_2\text{O}_3)-\text{CoO}-\text{MnO}_2$ system were investigated, where the amount of Bi_2O_3 , CoO, MnO_2 remains constant, around 0.2 mol%, TiO_2 is no more than 0.12 mol%, but Ti/Sb ratio was varied.

2. Experimental procedure

2.1. Sample preparation

Oxide precursors of 99.9% purity were used. Samples were prepared by conventional ceramic processing. Bi_2O_3 , TiO_2 , Sb_2O_3 were first mixed in specific proportions,

* Corresponding author.

E-mail address: cchzhang@263.net (C. Zhang).

where the total amount of the mixture and the amount of Bi_2O_3 remain constant, but the amount of TiO_2 and Sb_2O_3 were adjusted with Ti/Sb ratio (by weight) 1, 1.4, 2, 3, 5, respectively. The mixture was ball-milled for 48 h, air dried and sieved, then sintered at 650°C for 5 h. The pre-sintered mixtures of Bi_2O_3 , TiO_2 , Sb_2O_3 were mixed with ZnO , CoO and MnO_2 . The mixture was milled with agate balls and deionized water for 48 h. After being air-dried and sieved, the mixture was calcined at 750°C for 2 h. The calcined mixture was milled for another 24 h, air-dried and sieved. Finally the discs of 12 mm diameter were pressed and sintered at 1200°C for 2 h and cooled down to 800°C at a rate of $200^\circ\text{C}/\text{h}$. After lapping both surfaces, silver paste was coated on the surfaces by firing at 500°C .

2.2. Methods of characterization

For phase identification of the fired specimens, X-ray diffraction analysis (XRD) and an electron probe micro-analyzer (EPMA) were performed. Sintered density was determined by Archimede method. The microstructure and grain size distributions were carried out using a scanning electron microscope (JEOL JSM-35C). Grain size was measured by the linear intercept method on the micrographs. The polished samples were lightly etched with dilute solution of hydrochloric HCl ($\text{HCl}:\text{H}_2\text{O}=1:2$) for microstructure investigations.

Current–voltage (I–V) characteristics were measured in d.c. modes for lower current regions. The nonlinear coefficient α is evaluated in terms of relation:

$$\alpha = \frac{\ln I_2 - \ln I_1}{\ln V_2 - \ln V_1} \quad (1)$$

where V_2 and V_1 are the voltage corresponding to $I_2=10$ mA and $I_1=1$ mA.

The voltage-dependent capacitance at the pre-breakdown region was measured with the aid of an adjustable d.c. power supply. I–V measurements were made at room temperature with an LCR meter at 1 kHz in the bias range 0–30 V. d.c. Degradation phenomena of samples were performed under stabilized d.c. bias at 140°C for periods up to 120 h. The applied voltage ratio was $0.75 V_{1\text{ mA}}$ (i.e. 75% of the voltage when the current was 1 mA). When the leakage current increased to 200 μA , the tests were ceased.

3. Results and discussion

3.1. The effect of Ti/Sb ratio on the microstructure feature

The typical XRD patterns of the samples are shown in Fig. 1. They revealed that $\beta\text{-Bi}_2\text{O}_3$ and antimony spinel

exist as minor phases for the sample with Ti/Sb ratio of 2. As for the sample with the Ti/Sb ratio of 5, secondary phases were hardly detected on XRD patterns. However, small crystal particles are present at the triple point and also at the grain boundaries in the SEM observations. EPMA revealed that substantial Sb is present in these particles, and it also indicated higher Bi concentration at the grain boundary than in the grain interiors.

The sintered densities were in the range from 94–96%. Fig. 2 shows the microstructure of the samples. For the sample with Ti/Sb ratio of 2, the average grain size is 20 μm . Some ZnO grains have a single twin, which is characterized by one straight line. Secondary phases are seen mostly distributed near the grain-boundary. Grain size of the sample with Ti/Sb ratio of 5 is larger than those in Fig. 2(a) (the average grain size is 40 μm). Twinning is very uncommon and this is due to the small amount of Sb_2O_3 (0.025 wt.%) in this sample. In both cases, grain-boundaries are flat, and ZnO grains are plate-shaped and the corners are slightly rounded. These features indicate the least involvement of liquid phase during the sintering process.¹² Fig. 2(c) and (d) show the fractured surfaces of specimens with Ti/Sb ratio of 3 and 1.4, respectively. They reveal mainly polygon-shaped grains of anhedral morphology, and have average grain sizes 11, 9.0 μm , respectively. A lot of twin boundaries can be seen in the sample with a Ti/Sb ratio of 1.4 but not in the sample with a Ti/Sb ratio of 3; this is maybe due to the small amount of Sb_2O_3 (0.06 wt.%) in the latter. The microstructure of the specimen with a Ti/Sb ratio of 1 is very similar to that of the specimen with a Ti/Sb ratio of 1.4 except that the grain size is smaller (7.8 μm).

It should be pointed out that the twin boundaries observed here did not appear in every grain as reported by Senda and Bradt,⁴ the reason for which may be co-existence of TiO_2 and Sb_2O_3 in the original composition, or the small amount of Sb_2O_3 (<0.11 wt.%) in all the samples.

3.2. Electrical properties and degradation behavior

Fig. 3 shows $E_{1\text{mA}}$ and α changing with different Ti/Sb ratio. Both parameters have the same changing tendency with the Ti/Sb ratio. Fig. 5 shows the I–V characteristic of the samples. These results indicate that except for the sample with a Ti/Sb ratio of 2, the decrease of the Ti/Sb ratio causes an increase in the breakdown field and α -values, i.e., the breakdown field does not increase monotonically with an increase in the amount of Sb_2O_3 or a decrease in TiO_2 within the whole range. The specimen with a Ti/Sb ratio of 5 has the lowest breakdown field around 20 v/mm and a nonlinear coefficient of around 22. The sample with a Ti/Sb ratio of 2 has a lower breakdown field than that for the sample

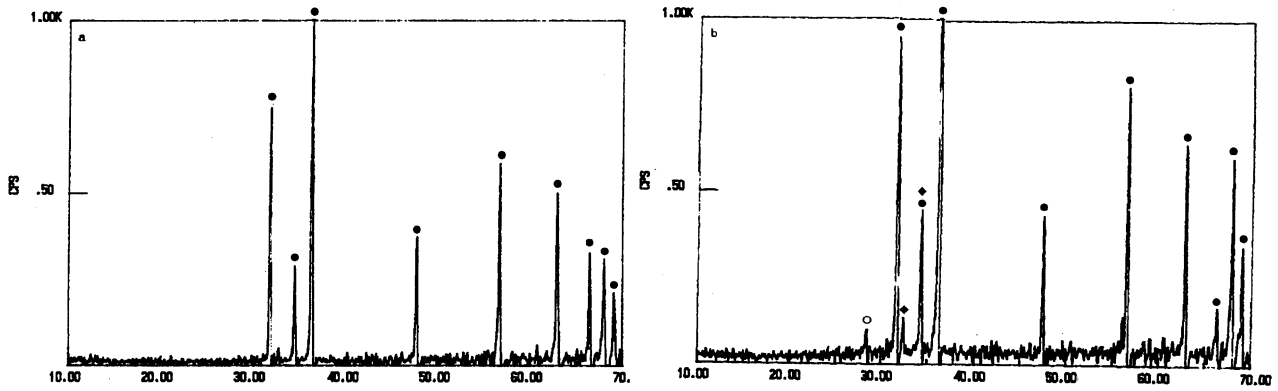


Fig. 1. XRD patterns of samples with Ti/Sb ratio; (a) 5 and (b) 2, respectively. ● — ZnO, ◆ — $\text{Zn}_7\text{Sb}_2\text{O}_{12}$, ○ — $\beta\text{-Bi}_2\text{O}_3$.

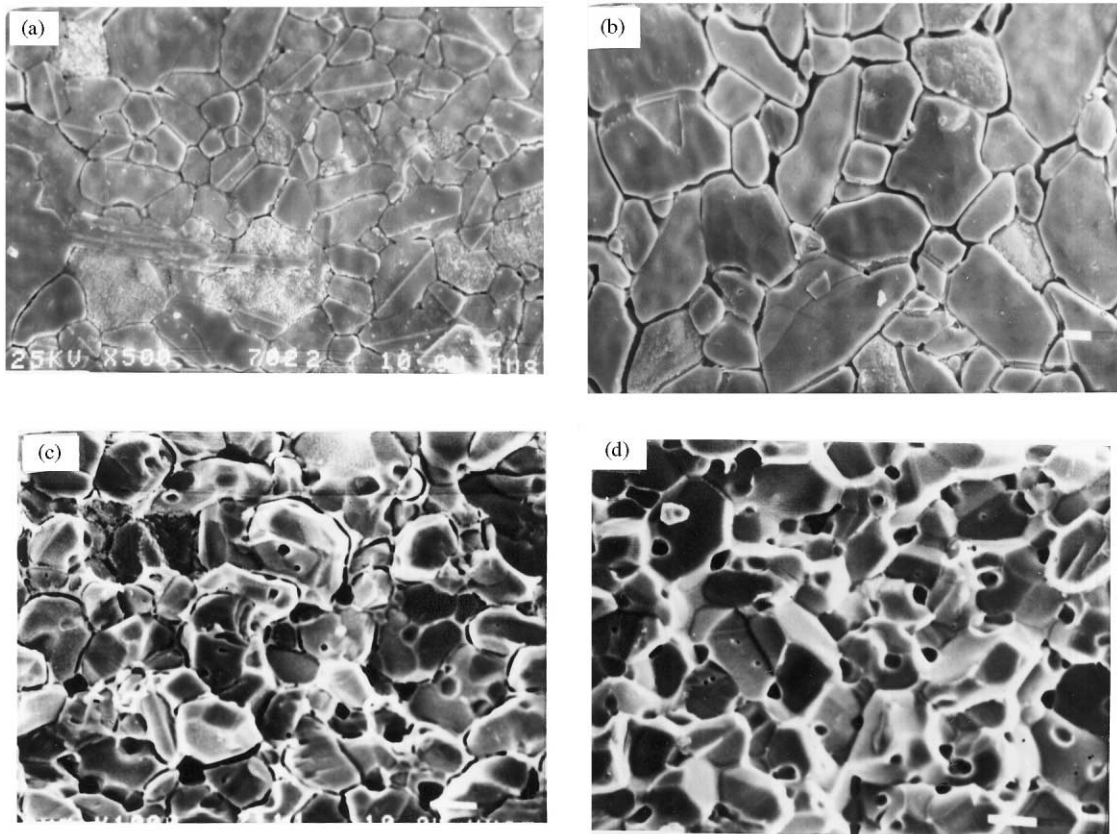


Fig. 2. SEM micrograph of ZnO ceramics, Ti/Sb ratio: (a) 2, (b) 5 (etched surface) (c) 3, (d) 1.4 (fractured surface). (Bar:0 μm).

with Ti/Sb ratio of 3. This can be explained as follows: there was inhomogeneity in the microstructure, and there was variation of electrical properties of the individual grain boundary, for example, there existed some ineffective grain-boundary.^{3,13} Although the twin boundary has the higher barrier voltage,¹⁰ it does not appear to form within each individual ZnO grain as there are a lot of grain boundaries without twinning that have the lower barrier voltage. Also, the broader grain size distribution resulted in a lower breakdown voltage and nonlinear coefficient.¹⁴ Here, SEM confirmed that there exists variations of grain size in all samples and the distribution of grain

size for the sample with a Ti/Sb ratio of 2 is broader than that for the sample with a Ti/Sb ratio of 3, the reason for which is related to the formation of the twin boundaries. As suggested by Senda and Bradt,⁴ twin boundary has the reduced mobility, however, for the grains without twinning, the grain growth is rapid, so the grain sizes differ greatly.

Combined with microstructure analysis in 3.1, it can be seen that Ti/Sb ratio plays a crucial role in the microstructure and electrical property of the studied system.

To define the stability of the sample, curves were plotted in terms of leakage current I_L against time (Fig. 4). If

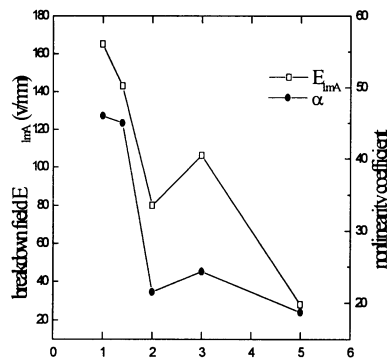


Fig. 3. Breakdown field and nonlinear coefficient vs. Ti/Sb ratio.

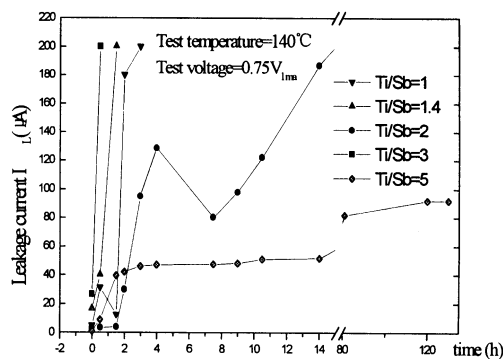


Fig. 4. d.c. Degradation behavior for samples of different Ti/Sb ratio.

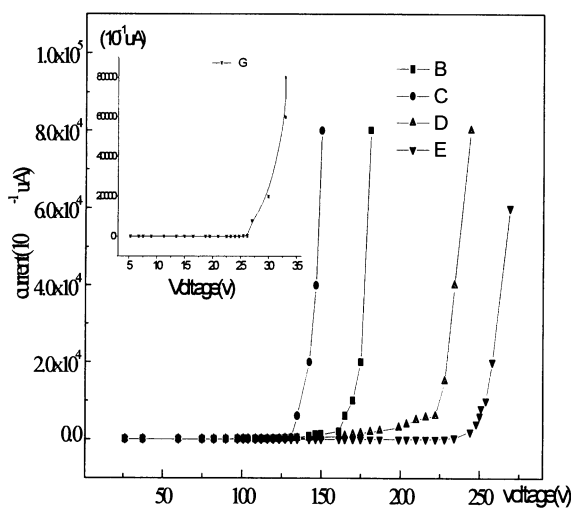


Fig. 5. I–V characteristic of sample with different Ti/Sb ratio: B-3, C-2, D-1.4, E-1, G (inset)-5.

the leakage current did not exceed 200 μA during 120 h, it could be concluded the specimen had good stability. Fig. 4 revealed that the leakage current increased with the biasing time. The defect model proposed by Gupta and Carlson^{6(b)} can be used to explain these results. The basic concept of this model is that the Schottky barrier consists of two components in the depletion layer: a

stable component consisting of spatially fixed positively charged ions and a metastable component consisting of mobile zinc interstitials in the depletion layer. Under external stress, zinc interstitials in the depletion layer are driven to migrate toward the grain boundary interface to react with the negatively charged V'_{Zn} , and neutral defects are formed at the interface. The barrier heights and the width of the depletion layer are thus continually reduced by the decreasing metastable component through the decreasing concentration of Zn interstitials by diffusion and chemical reaction.^{6(b)} This is confirmed by the following results in Table 1. It was reported that relation between I_L and $t^{1/2}$ obey an empirical equation (linear relation).⁷

$$I_L = I_{L0} + k\sqrt{t} \quad (2)$$

Where I_L is the leakage current at time t , I_{L0} is the leakage current at $t=0$ and k is the rate constant. However, in our experiments, it seems that the exponent of t for sample with a Ti/Sb ratio of less than 5 is more than 0.5. For the samples with a Ti/Sb ratio of 1, 1.4 and 3, leakage current increased rapidly with time and soon surpassed measurement range, i.e., they had higher degradation rates (see Fig. 4). However, two other samples were quite stable and relatively temperature insensitive in the operating region of interest. The sample with a Ti/Sb ratio of 5 had a lower breakdown field and improved degradation characteristics. According to the model of Gupta,^{6(b)} the difference in the degradation rates was maybe related to the defects and their distribution in the samples. The exact cause needs further study.

3.3. Capacitance-voltage (*c-v*) analyses/Grain-boundary property

On the basis of Schottky barrier model for the grain boundary region, parameters such as the barrier height, donor density, interface state density and depletion layer width have been determined from the capacitance–voltage relations.⁸

$$\left(\frac{1}{c} - \frac{1}{2c_0}\right)^2 = 2(\phi_b + V)/qN_d\epsilon \quad (3)$$

where

$$1/2c_0 = (2\phi_b/qN_d\epsilon)^{1/2} \quad (4)$$

q is the electron charge, ϵ the dielectric constant of ZnO, N_d the donor density, ϕ the barrier height, c the capacitance per grain boundary junction and V the applied voltage per grain boundary. Using these values the depletion layer width (w) can be obtained from the equation:

Table 1
Grain boundary properties of ceramics from C–V data^a

Ti/Sb ratio	N_d ($\times 10^{24} \text{ m}^{-3}$)	ϕ_b (eV)	N_s ($\times 10^{16} \text{ m}^{-2}$)	W ($\times 10^{-8} \text{ m}$)
1	2.373	1.5648	6.0270	2.5390
1.4	2.049	1.5149	5.5094	2.6886
2	0.835	1.1574	3.0691	3.6876
3	1.553	2.6282	6.3187	4.0671
5	2.099	2.2802	6.8407	3.2594
5 ⁺	1.501	1.3830	4.5057	3.0014

^a + measured after d.c. degradation.

$$w = (2\varepsilon\varepsilon_0\phi_b/q^2N_d)^{1/2} \quad (5)$$

where ε_0 is the permittivity of the vacuum. The density of states at the interface (N_s) between the ZnO grain and the grain boundary region can be estimated from

$$N_s = (2N_d\varepsilon\varepsilon_0\phi/q)^{1/2} \quad (6)$$

Table 1 summarizes the grain boundary properties of the specimens sintered under identical conditions. The donor density is of the same order, which is indicative of the condition prevailing in the grain interiors by way of the concentration of n -type defects as well as the donor impurities (Ti^{4+} in the present case). The specimen with a Ti/Sb ratio of 2 has the lowest values of N_s , N_d and ϕ_b . The reason for which may be the presence and concentration of bismuth, and probably other dopant atoms residing in the grain boundary alter the grain boundary property. It can be seen that ϕ_b is reduced after degradation.

4. Conclusion

Ti/Sb ratio in ZnO ceramics doped with both TiO_2 and Sb_2O_3 greatly influences their microstructure and electrical properties. Grain size does not decrease monotonically with the decrease of Ti/Sb ratio, i.e., the increase of Sb_2O_3 content and decrease of TiO_2 content. It reveals that TiO_2 and Sb_2O_3 dopants have a synergistic effect on the ZnO varistor: the formation of twin boundary is related to the Ti/Sb ratio. When Ti/Sb ratio is decreased to 2, twin boundaries appear to form in ZnO grains, which result in the broad grain size distribution and reduce the average breakdown field of this sample. Under the same processing conditions, low-voltage varistor with

excellent electrical characteristics and good degradation stability can be obtained by a correct Ti/Sb ratio of 5.

Acknowledgements

The author gratefully acknowledges the access to EPMA provided by Dr. Liangfang in the State key Laboratory for advanced material in WUST.

References

1. Inada, M., Formation mechanism of nonohmic zinc oxide ceramics. *Jpn. J. Appl. Phys.*, 1980, **19**, 409–419.
2. Bernik, S., Zupancic, P. and Kolar, D., Influence of $\text{Bi}_2\text{O}_3/\text{TiO}_2$, Sb_2O_3 and Cr_2O_3 doping on low-voltage varistor ceramics. *J. Eur. Ceram. Soc.*, 1999, **19**, 709–713.
3. Bowen, L. J. and Avella, F. J., Microstructure, electrical properties and failure prediction in low-clamping voltage zinc oxide varistors. *J. Appl. Phys.*, 1983, **54**(5), 2764–2772.
4. Senda, T. and Bradt, R. C., Grain growth of ZnO during the sintering of $\text{ZnO-Sb}_2\text{O}_3$ ceramics. *J. Am. Ceram. Soc.*, 1991, **74**, 1296–1302.
5. Bruley, J., Bremer, U. and Krasevec, V., Chemistry of basal plane defects in $\text{ZnO-Sb}_2\text{O}_3$ ceramics. *J. Am. Ceram. Soc.*, 1992, **75**(11), 3127–3128.
6. Trontelj, M., Kolar, D. and Krasevec, V., Influence of additives on varistor microstructure, pp. 107–116. Gupta T. K. and Carlson, W. G., Defect-induced degradation of barrier in ZnO varistor, pp. 30–40. In *Advances in ceramics*, vol. 7, ed. M. F. Yan and A. Hauer. Am. Ceram. Soc., Columbus, OH, 1983.
7. Fan, J. and Freer, R., Improvements of the nonlinearity and degradation behavior of ZnO varistors. *Br. Ceram. Trans.*, 1993, **92**(6), 221–256.
8. Mukae, K., Tsuda, K. and Nagasawa, I., Capacitance-v.s-voltage characteristics of ZnO varistors. *J. Appl. Phys.*, 1979, **50**(6), 4475–4476.
9. Suzuki, H. and Bradt, R. C., Grain growth of ZnO in $\text{ZnO-Bi}_2\text{O}_3$ ceramics with TiO_2 additives. *J. Am. Ceram. Soc.*, 1995, **78**(5), 1354–1360.
10. Haskell, B. A., Souri, S. J. et al., Varistor behavior at twin boundary in ZnO varistors. *J. Am. Ceram. Soc.*, 1999, **82**(8) 2106–2110.
11. Ezhilvalavan, S. and Kutty, T. R. N., Effect of antimony oxide stoichiometry on the nonlinearity of ZnO varistor ceramics. *Mater. Chem. Phys.*, 1997, **49**, 258–269.
12. Rahaman, M. N., *Ceramic Processing and Sintering*. Marcel Dekker, Inc., New York, 1995 p. 520–521.
13. Wang, H., Li, W. and Cordaro, J. F., Single junctions in ZnO varistors studied by current-voltage characteristics and deep level transient spectroscopy. *Jpn. J. Appl. Phys.* 1995, **34**(Part 1, NO.4A) 1765–1771.
14. Nan, C. W. and Clarke, D. R., Effects of variations in grain size and grain boundary barrier heights on the current-voltage characteristics of ZnO varistors. *J. Am. Ceram. Soc.*, 1996, **79**(12), 3185–3192.